REPORT DOCUMENTATION PAGE

Form Approved
OMB No. 0704-0188

1. REPORT DATE *(DD-MM-YYYY)*

2. REPORT TYPE
Briefing Charts

3. DATES COVERED *(From - To)*

4. TITLE AND SUBTITLE
Dynamics of High Pressure Reacting Shear Flows

5a. CONTRACT NUMBER

5b. GRANT NUMBER

5c. PROGRAM ELEMENT NUMBER

6. AUTHOR(S)
David Forliti (Sierra Lobo); Jeff Wegener (UCLA); Ivett Leyva (AFRL)
Doug Talley (AFRL)

5d. PROJECT NUMBER

5e. TASK NUMBER

5f. WORK UNIT NUMBER
Q0YA

7. PERFORMING ORGANIZATION NAME(S) AND ADDRESS(ES)

Air Force Research Laboratory (AFMC)
AFRL/RQRC
10 E. Saturn Blvd
Edwards AFB, CA, 93524

8. PERFORMING ORGANIZATION REPORT NO.

9. SPONSORING / MONITORING AGENCY NAME(S) AND ADDRESS(ES)

Air Force Research Laboratory (AFMC)
AFRL/RQR
5 Pollux Drive
Edwards AFB, CA, 93524

10. SPONSOR/MONITOR'S ACRONYM(S)

11. SPONSOR/MONITOR'S REPORT NUMBER(S)
AFRL-RQ-ED-VG-2013-171

12. DISTRIBUTION / AVAILABILITY STATEMENT
Approved for public release; distribution unlimited

13. SUPPLEMENTARY NOTES
Presented at AFOSR Space Propulsion and Power Contractor's meeting, Arlington, VA, Dec 17, 2013
PA Case Number: 13554; Clearance Date: Dec 10, 2013.
The U.S. Government is joint author of the work and has the right to use, modify, reproduce, release, perform, display, or disclose the work.

14. ABSTRACT

Briefing charts presented at AFOSR Space Propulsion and Power Contractor's Meeting, Arlington, VA, December 17, 2013.

15. SUBJECT TERMS

16. SECURITY CLASSIFICATION OF: a. REPORT	b. ABSTRACT	c. THIS PAGE	17. LIMITATION OF ABSTRACT	18. NUMBER OF PAGES	19a. NAME OF RESPONSIBLE PERSON
Unclassified	**Unclassified**	**Unclassified**	SAR	31	Doug Talley
					19b. TELEPHONE NO *(include area code)* 661 275-6174

Standard Form 298 (Rev. 8-98)
Prescribed by ANSI Std. 239.18

Dynamics of High Pressure Reacting Shear Flows

David Forliti, Sierra Lobo, Inc.

Jeff Wegener, UCLA

Ivett Leyva, AFRL

Doug Talley, AFRL

Outline

- **Past results and current status of AFRL work**
  - Non-reacting review
  - Reacting flow facility description
  - Hot-fire testing preliminary results
- **New variable descriptions**
  - Dimensionless forcing frequency
  - Dimensionless forcing amplitude
- **Shakedown cold flow data**
- **Description of interaction mechanisms**

Goals

- **Extend previous non-reacting research on subcritical and supercritical acoustic-jet interactions to reacting flow in a canonical coaxial shear flow configuration**
  - Emphasis on the flame holding region
- **Maintain traceability to non-reacting conditions to assess the magnitude of the effect of chemical reactions**
- **Explore inter-element effects**

PAST APPROACH

- **Continue non-reacting research during construction of the reacting facility**

Where we were last year (steady)

Subcritical (Pr=0.44)

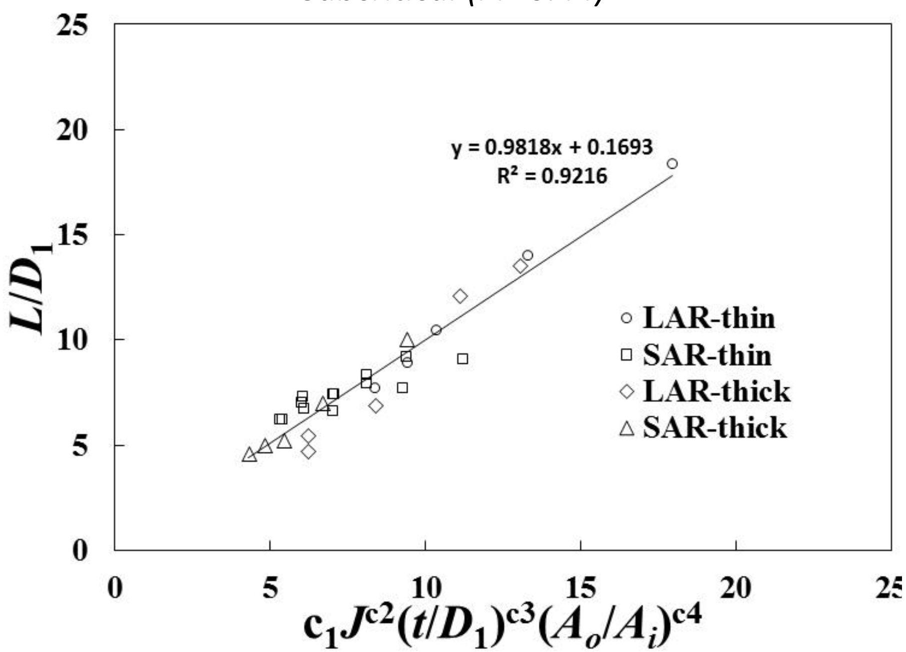

Supercritical (Pr=1.05)

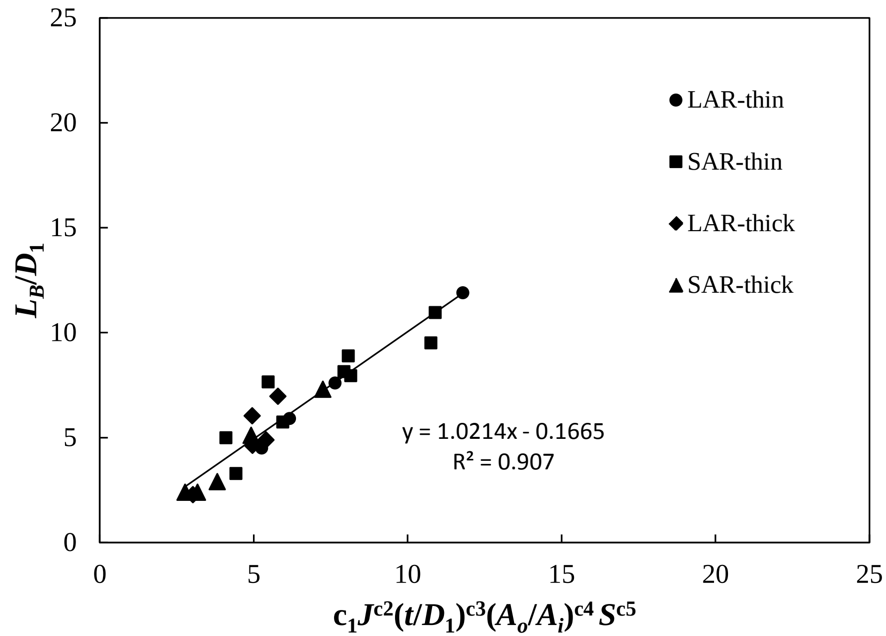

- *Correlated effects of momentum flux ratio, density ratio, and geometry on dark core length*

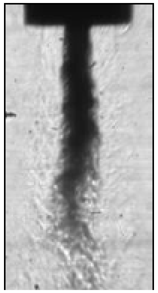

$$\left(\frac{L}{D_1}\right) = c_1 J^{c2}\left(\frac{t}{D_1}\right)^{c3}\left(\frac{A_o}{A_i}\right)^{c4}\left(\frac{\rho_{OJ}}{\rho_{IJ}}\right)^{c5}$$

P_r	c_1	c_2	c_3	c_4	c_5
0.44	9	-0.34	-0.15	0.30	
1.05	4.6	-0.42	-0.20	0.07	-0.29

Where we were last year (acoustics)

Three main classes of interactive behavior, each with major sub-classes

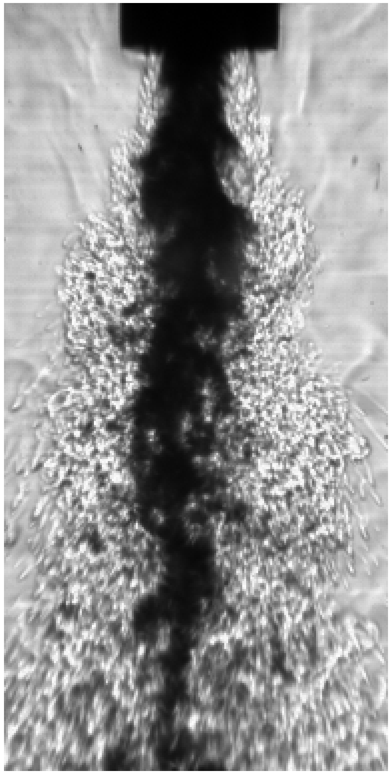

Pressure coupled

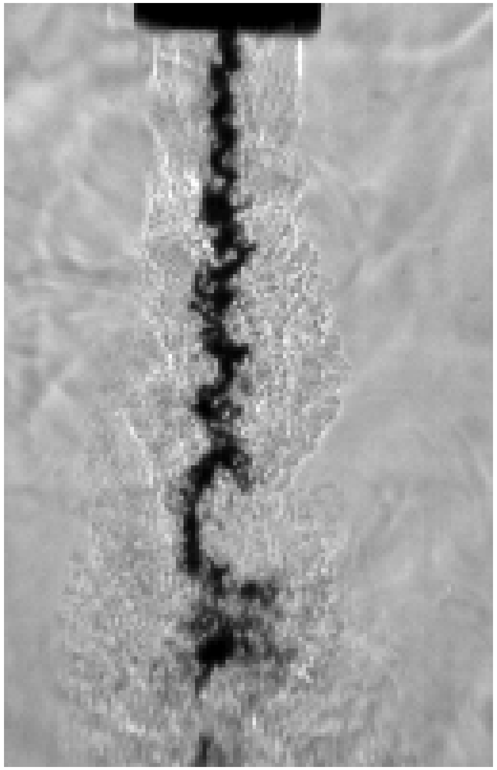

Velocity coupled

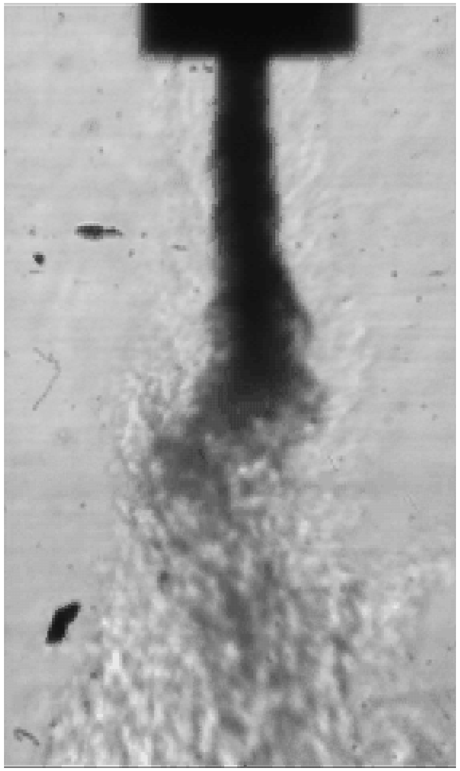

Little noticeable response

An extreme case

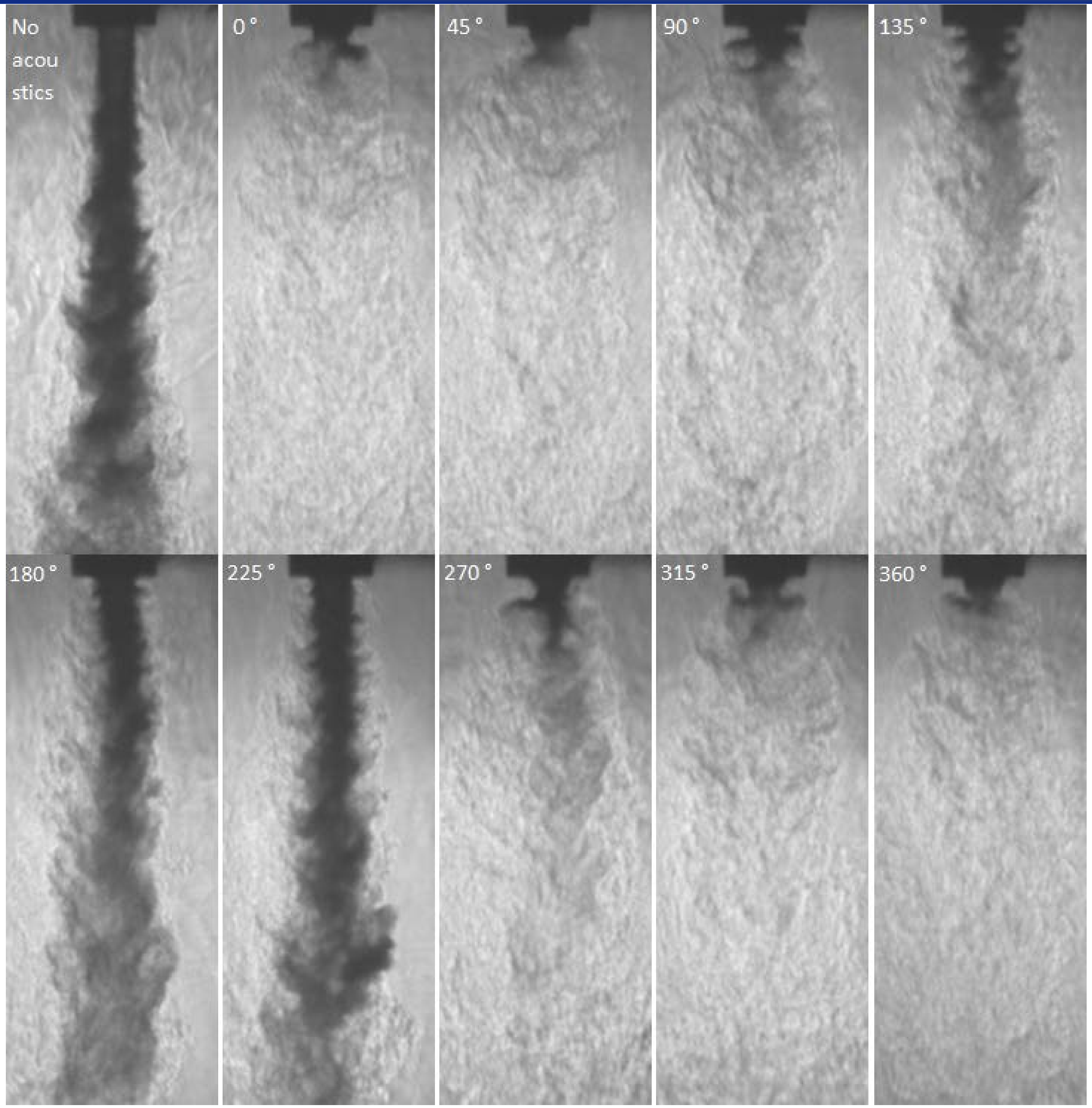

Pr=1.05, J=1.7

Annihilation of the dark core near pressure antinodes

Where we said we would be this year

Task	Date
Data Acquisition and Control System Final Check out	Sept 22-30, 2012
Inner chamber fabrication	Now- until December 1, 2012
System Check-out runs	October 2012- February 2013
Heat Exchanger Acceptance Testing	Jan-13
Cold Flow Runs	March - April 2013
Igniter Tests	May-June, 2013
First Hot-fire Data	Aug-Sept, 2013

First LOX/H2 combustion achieved in October 2013

Before

After

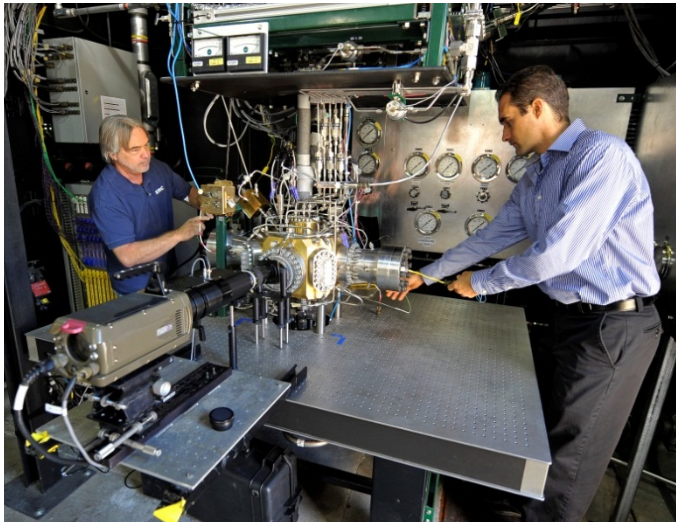

PA#13554

OH* emission at 400 psia

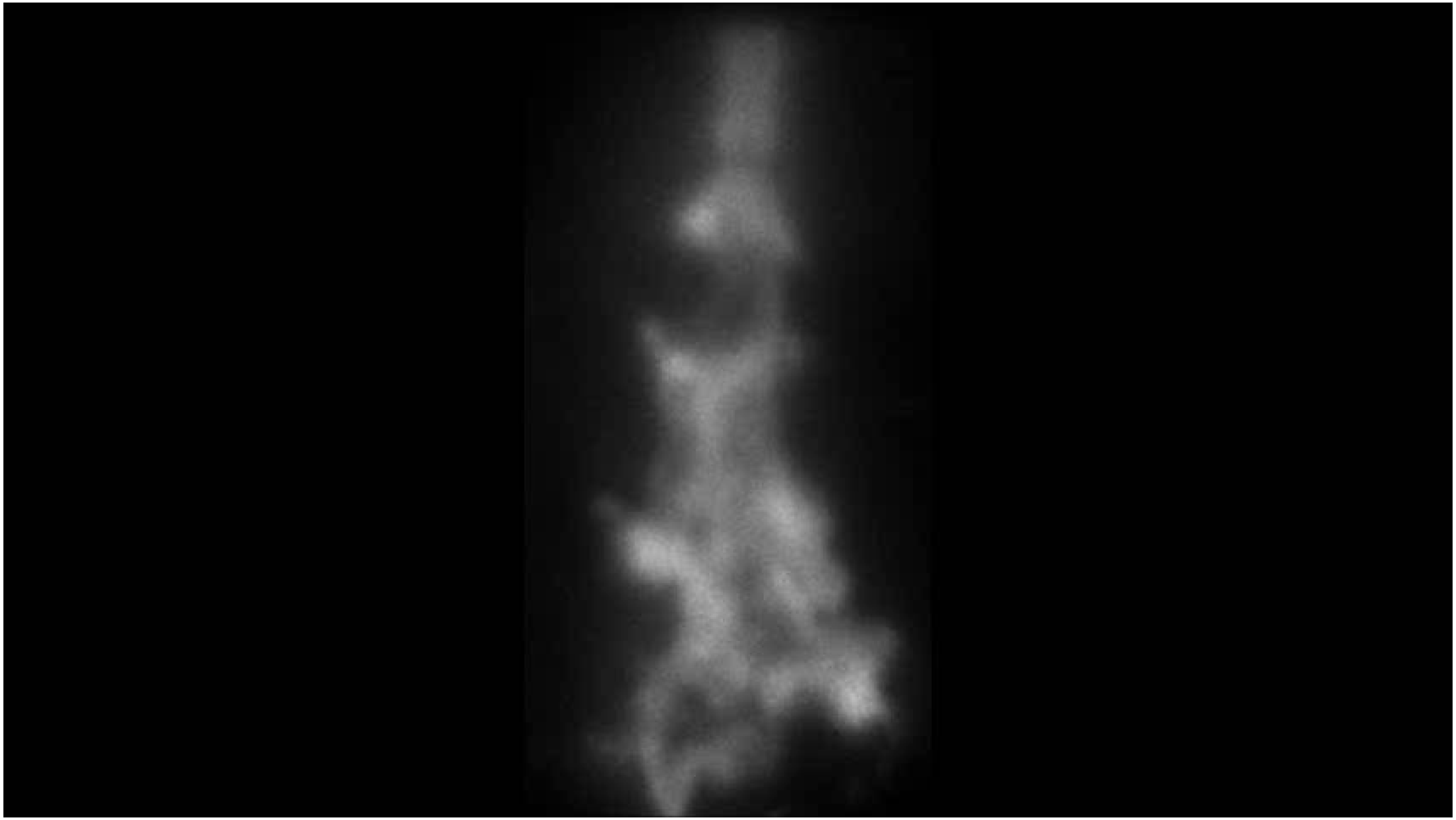

Features of the experimental facility

- **Complete control of acoustic phase**
  - Pressure node to pressure antinode and all phases in between
- **Precise control of amplitude**
  - No reliance on feedback from combustion to acoustics
- **Precise control of pressure**
  - Subcritical and supercritical
  - Pressurized externally in a large volume, little influence of combustion
- **Precise control of LOX temperature to within 1K**
  - Large sensitivity to temperature near the critical pressure
- **Completely new method of ignition for simplicity and operability at high pressures**

Nanotube photo ignition method

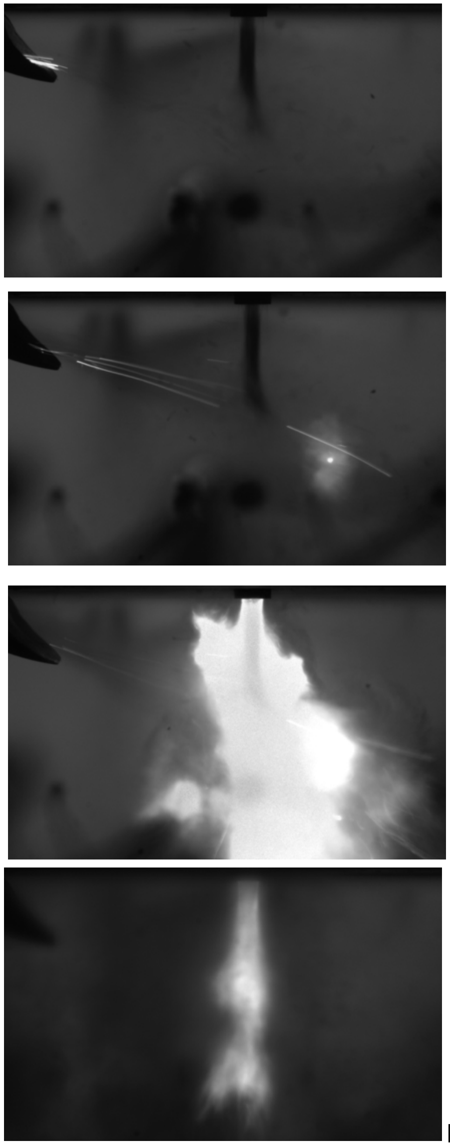

Carbon nanotube capsule

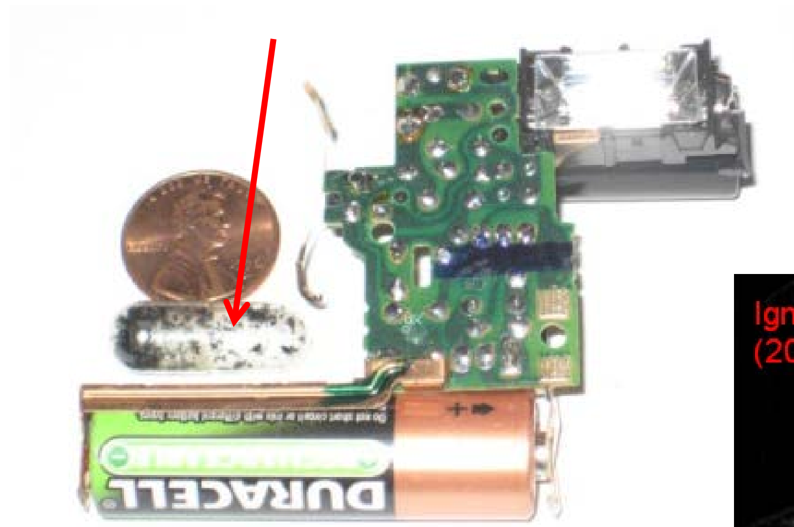

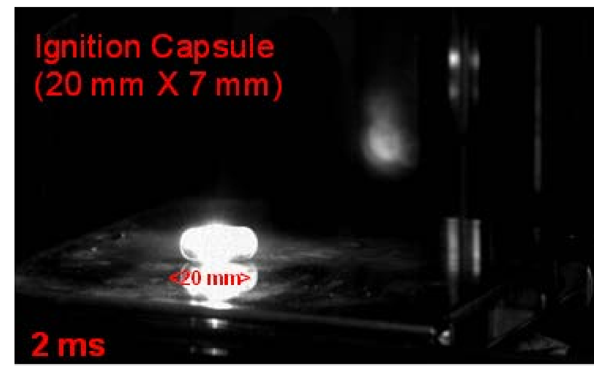

Original development under AFOSR funding from Mike Berman

Developed into a high pressure igniter under Mitat Birkan

Coaxial Jets

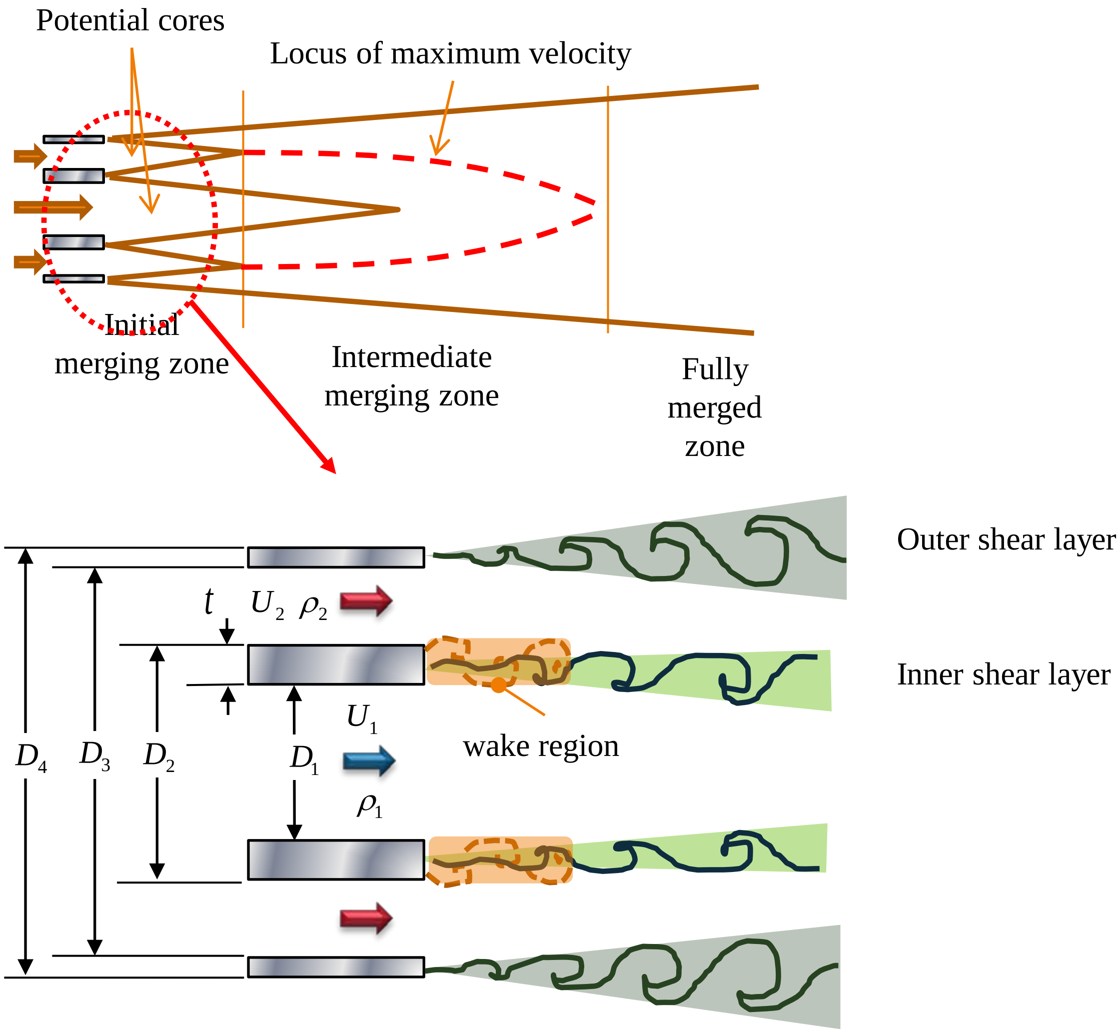

Geometry parameters

Area ratio

$$AR = \frac{D_3^2 - D_2^2}{D_1^2}$$

Dimensionless post thickness

$$\frac{t}{D_1}$$

Flow parameters

$$\mathrm{Re}_i = \frac{\rho_1 U_1 D_1}{\mu_1} \qquad \mathrm{Re}_i = \frac{\rho_2 U_2 (D_3 - D_2)}{\mu_2}$$

$$J = \frac{\rho_2 U_2^2}{\rho_1 U_1^2} \qquad r = \frac{U_2}{U_1}$$

$$s_1 = \frac{\rho_2}{\rho_1} \qquad s_2 = \frac{\rho_3}{\rho_2}$$

Inflow boundary conditions

- Mean velocity profiles
- RMS fluctuation profiles
- Spectral content

Forced Coaxial Jets

1. **Transverse Acoustic mode from chamber/siren**
   – f=f(c, geometry)
2. **Acoustic modes propellant lines**
   – f~c/2L
3. **Post wake**
   – $St=ft/U_{ch}$
4. **Shear layer instabilities**
   – $St_{\theta}=f\theta/U_{ch}$
5. **Jet preferred modes**
   – $St=fD_{ij}/U_{ij}$

Very low density ratio regime: $0.005 < \dfrac{\rho_2}{\rho_1} < 0.1$

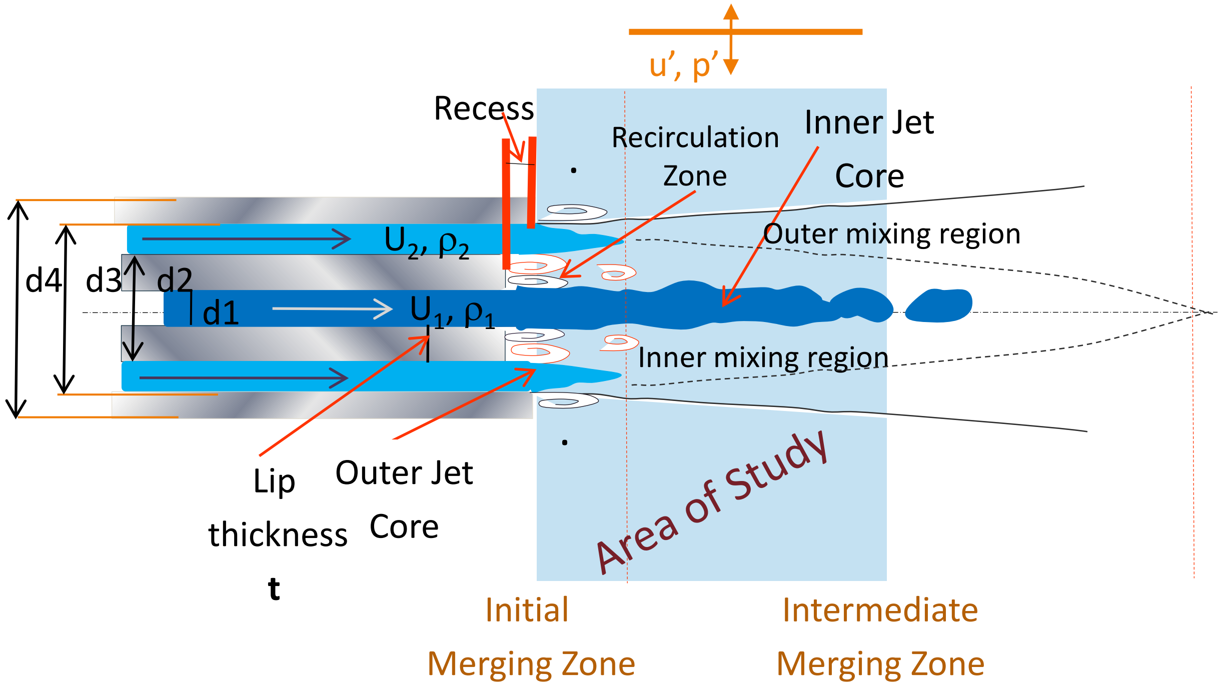

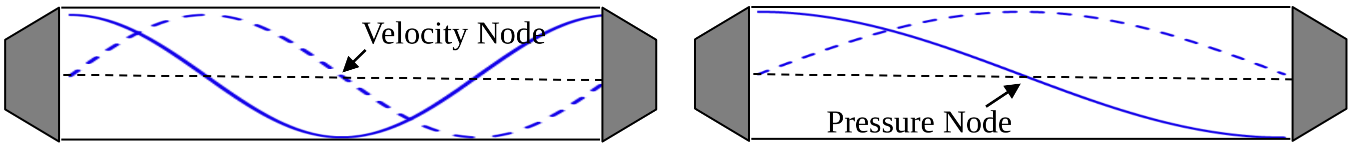

New Forcing Characterization

- **Shift pressure normalization from chamber pressure to injector dynamic pressure**

$$P'/\overline{P}_c \rightarrow \frac{P'}{\rho U^2/2}$$

- **Identify receptivity inception point—threshold for coupling between acoustics and flame**

$$F = \frac{f_{forcing}}{f_{jet}} \qquad A = \frac{p'}{\frac{1}{2}\rho U^2}$$

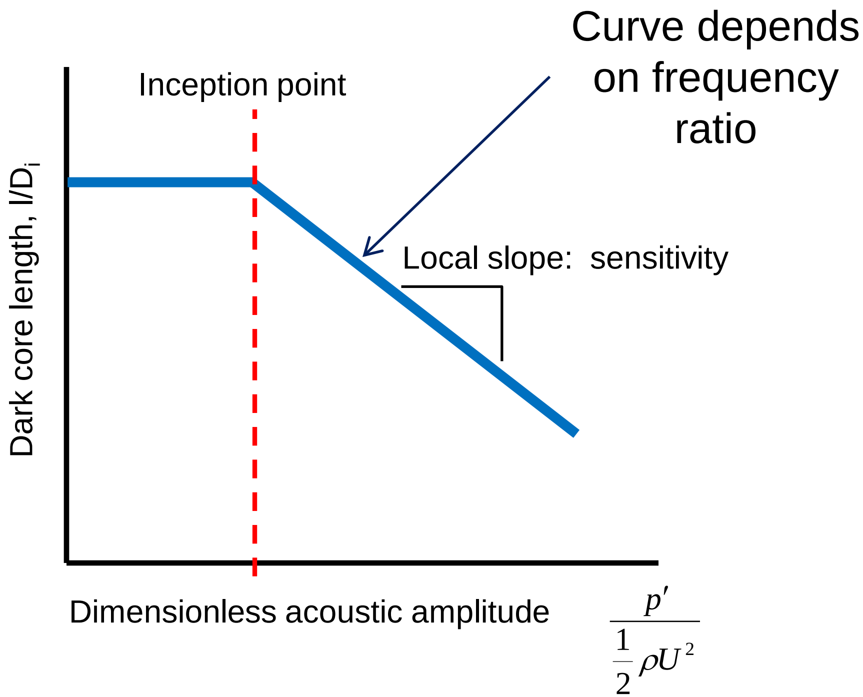

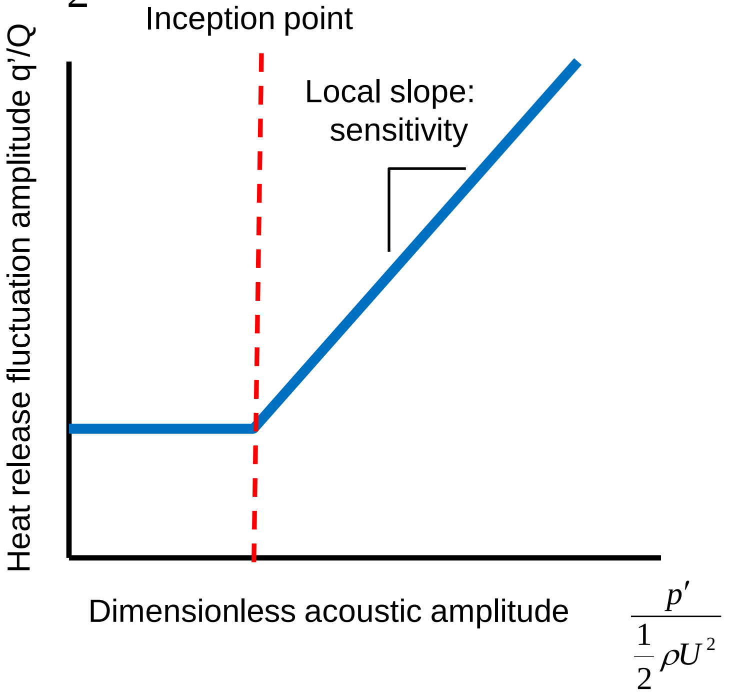

Characteristic Jet Frequencies

From Yule (1978), St ~ 0.3-0.4

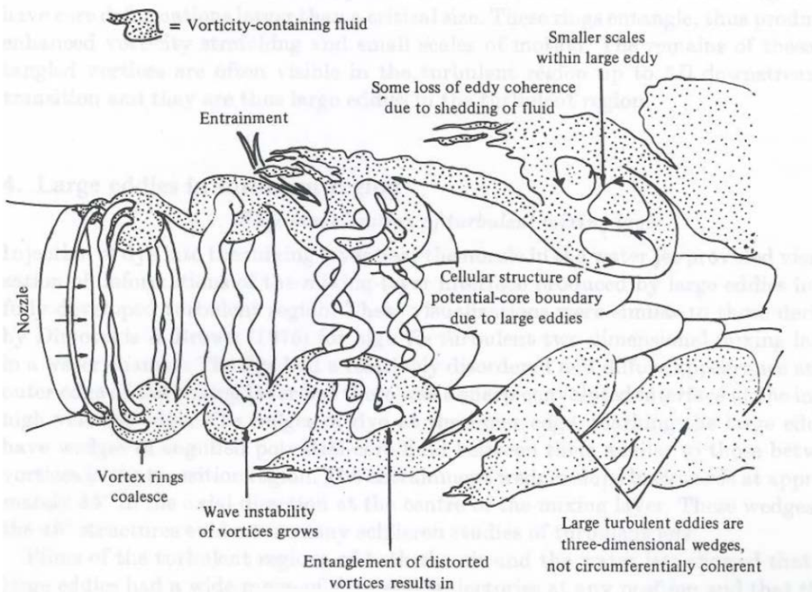

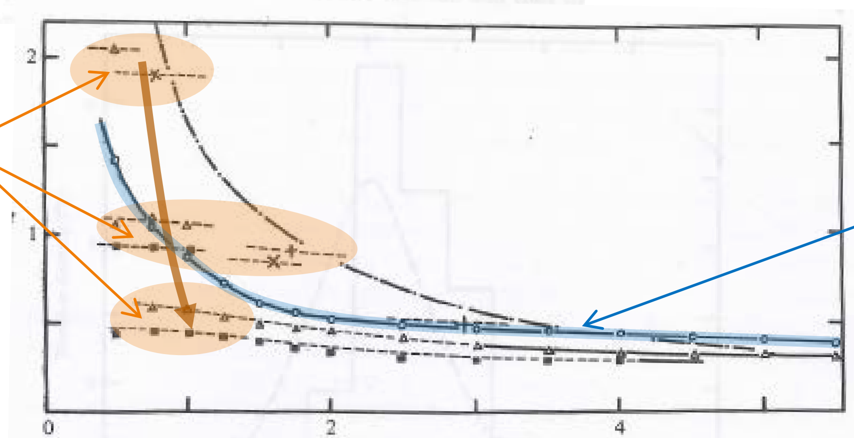

From Crow and Champagne (1971)

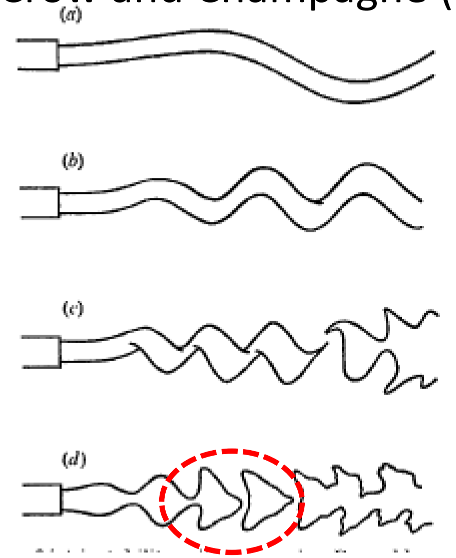

St ~ 0.3

Coaxial Jet Frequencies

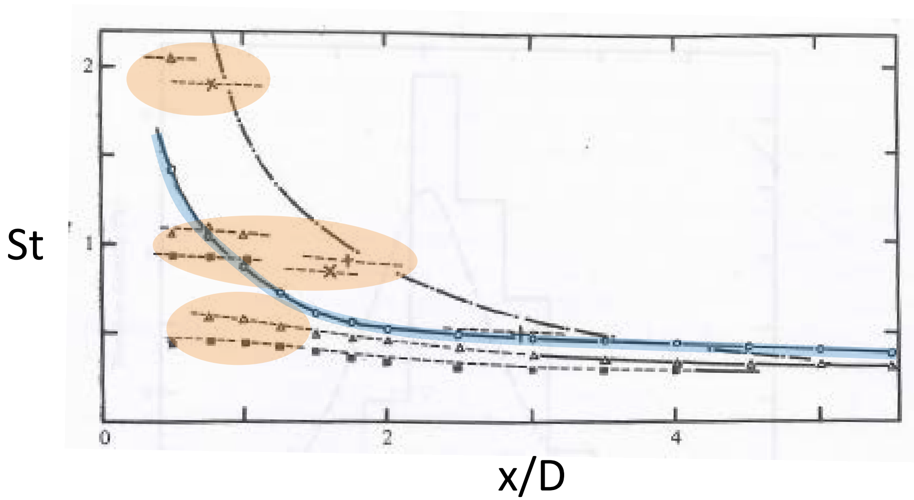

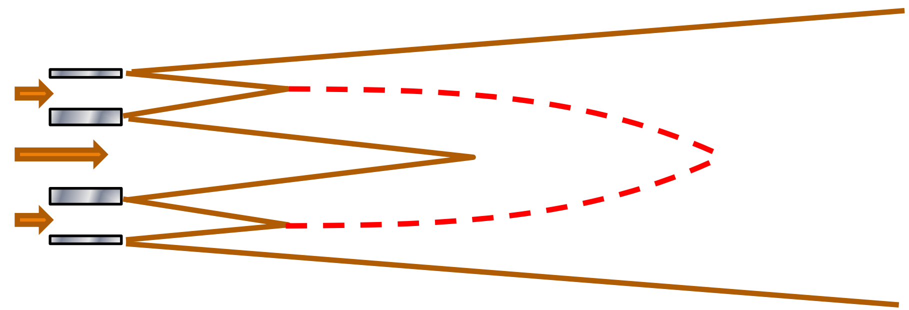

Phenomena that govern spectral features of coaxial jets

- Two shear layers exhibiting unique streamwise frequency distribution
- One shear layer driving the other (Dahm, Frieler, and Tryggvason 1992)
- Inner post wake instability
- Inflow turbulence
- Hydrodynamics where the shear layers merge (i.e. end of potential cores)
- Instabilities associated with two-phase flow (i.e. We number effects)

Unforced Coaxial Jets

- **Frequencies, convection velocities**

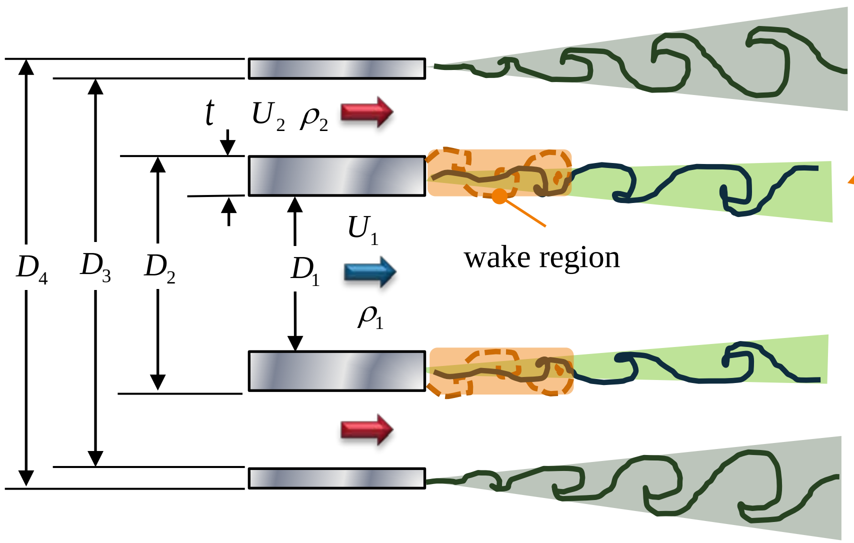

$$Umean_{Dimotakis} = \frac{U_o \rho_0^{1/2} + U_i \rho_i^{1/2}}{\rho_0^{1/2} + \rho_i^{1/2}}$$

Ko and Davies (free jet, 1971)

Ko and Kwan (inner shear layer of coaxial jet, 1971)

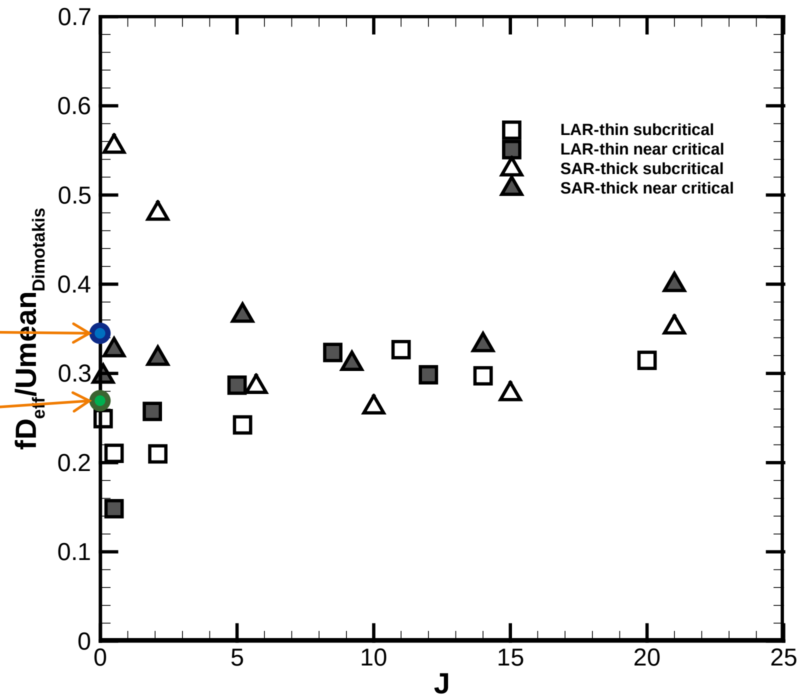

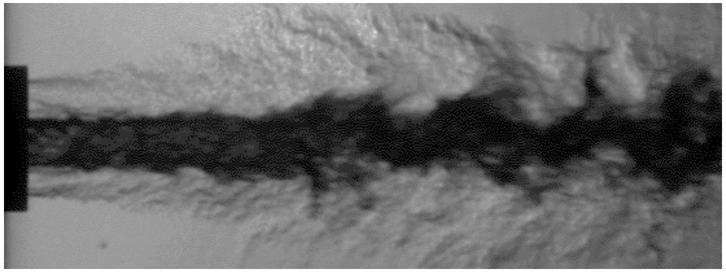

Shakedown Data

- **Cold flow data collected during facility shakedown**
  - Demonstrate operation of facility components
  - Identify delay times necessary to develop ignition sequence
  - Generate supporting evidence for Strouhal number scaling law
  - Explore sensitivity of receptivity to frequency and amplitude ratio

Select cold flow cases that have corresponding reacting flow conditions.

Unforced Coaxial Jets

J = 2.0

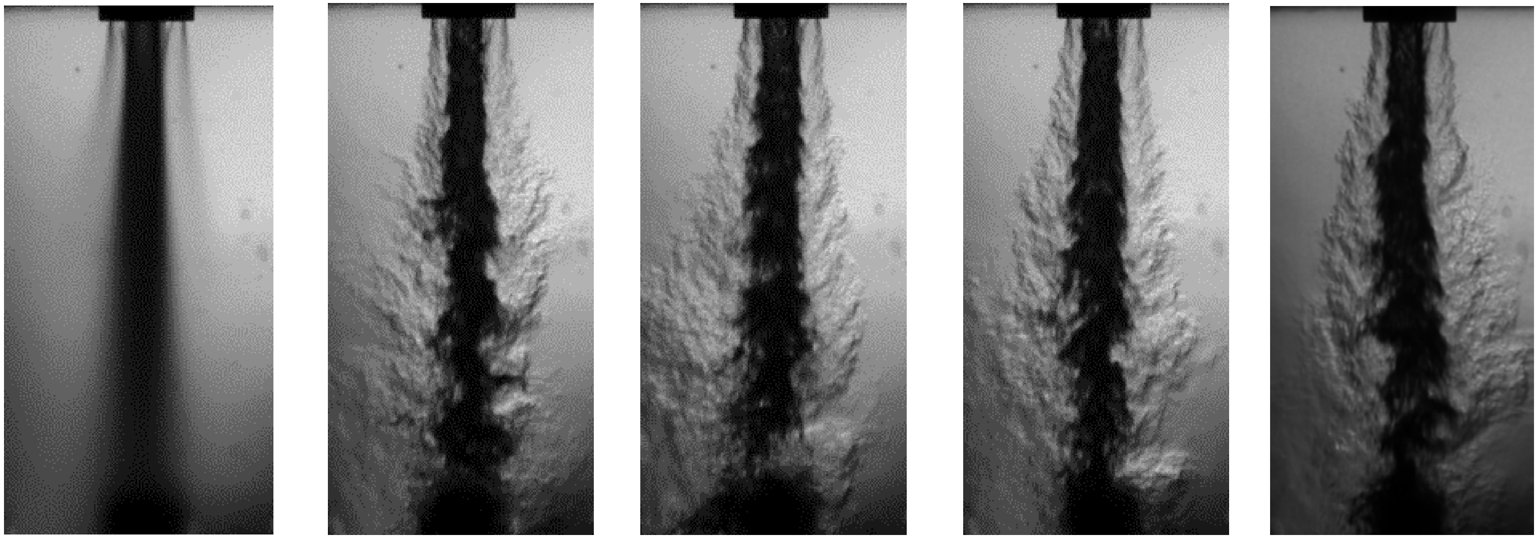

J = 6.0

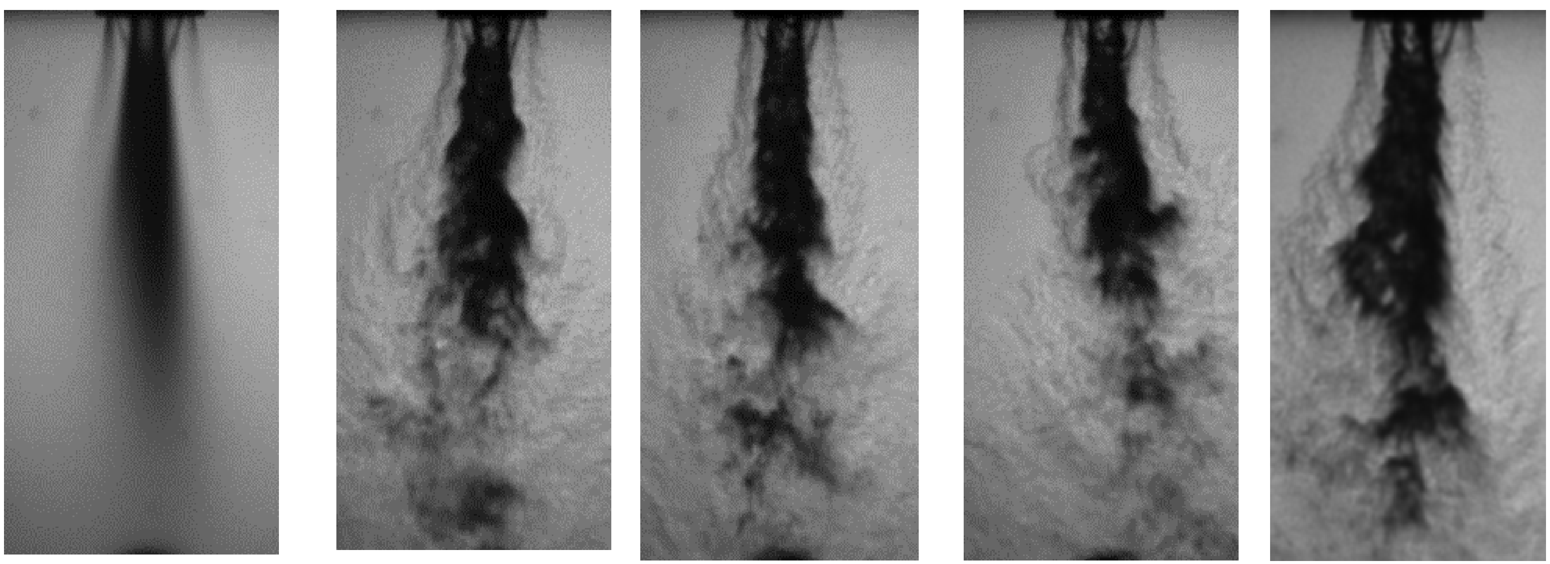

Convection Velocity

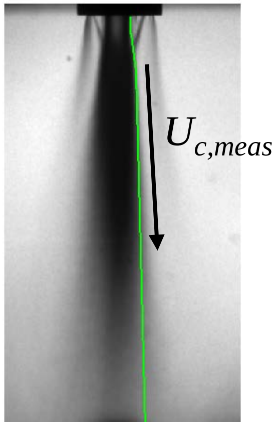

Verify the accuracy of the Dimotakis (1986) expression for shear layer convection velocity for these flow conditions.

$$U_{c,meas} = \frac{\Delta s}{\Delta t}$$

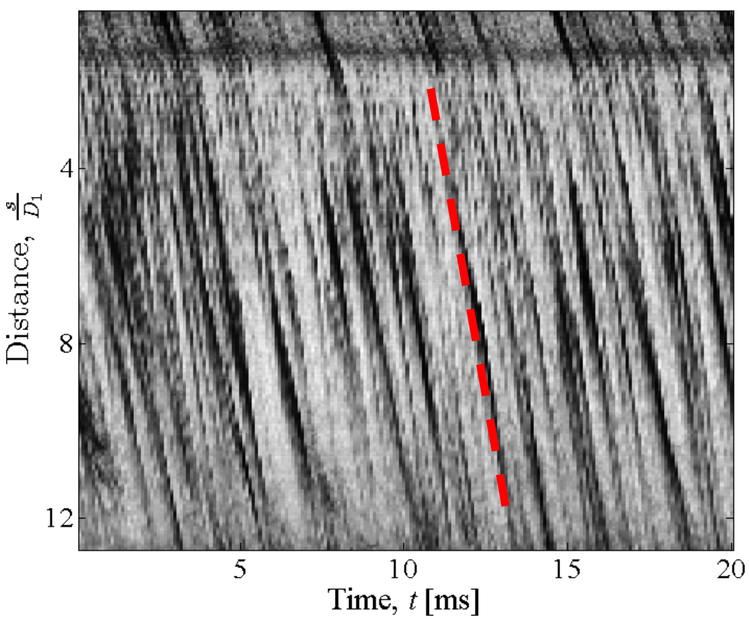

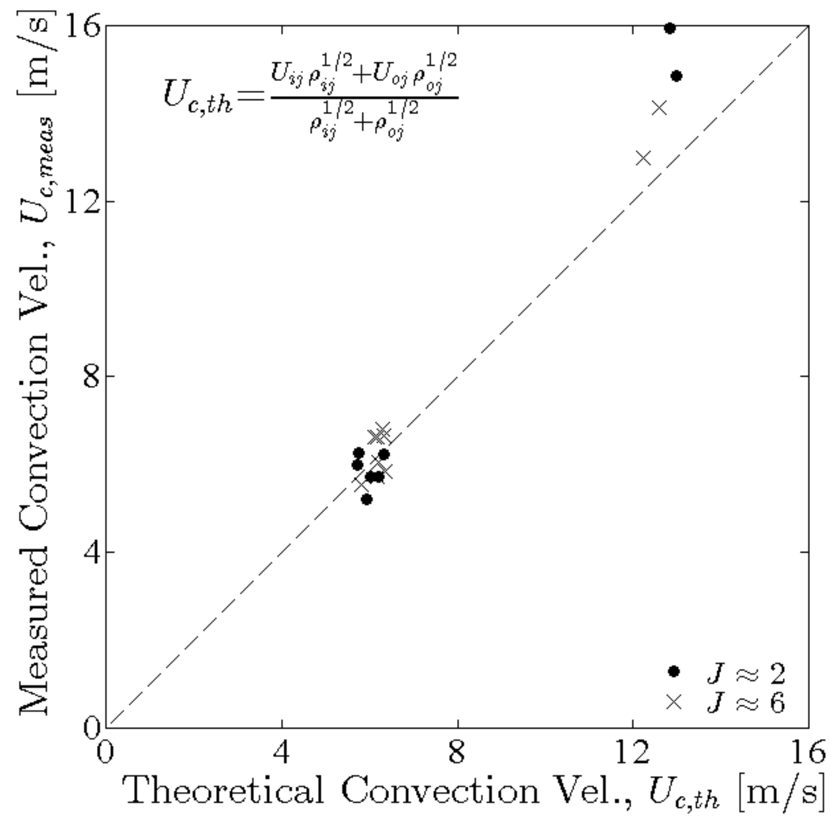

Preferred Mode Frequency

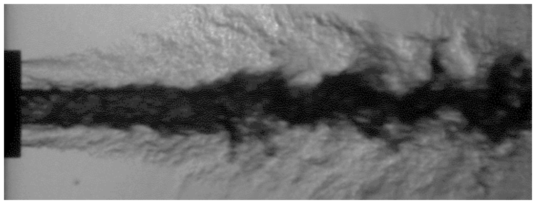

Most energetic convective mode pair from POD

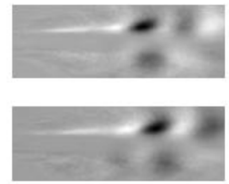

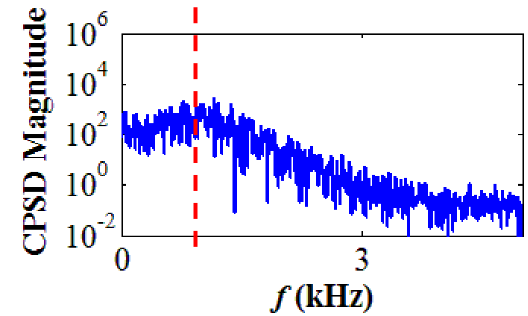

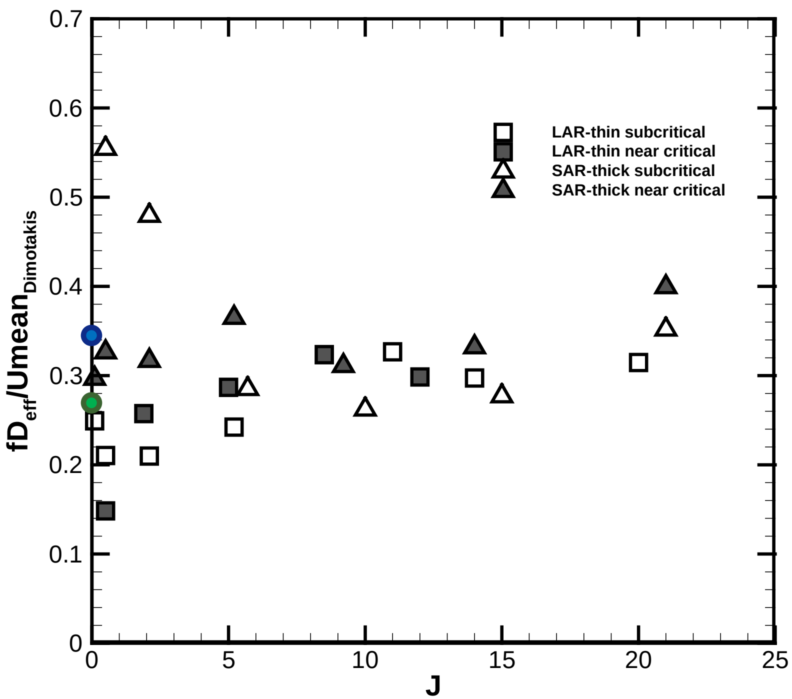

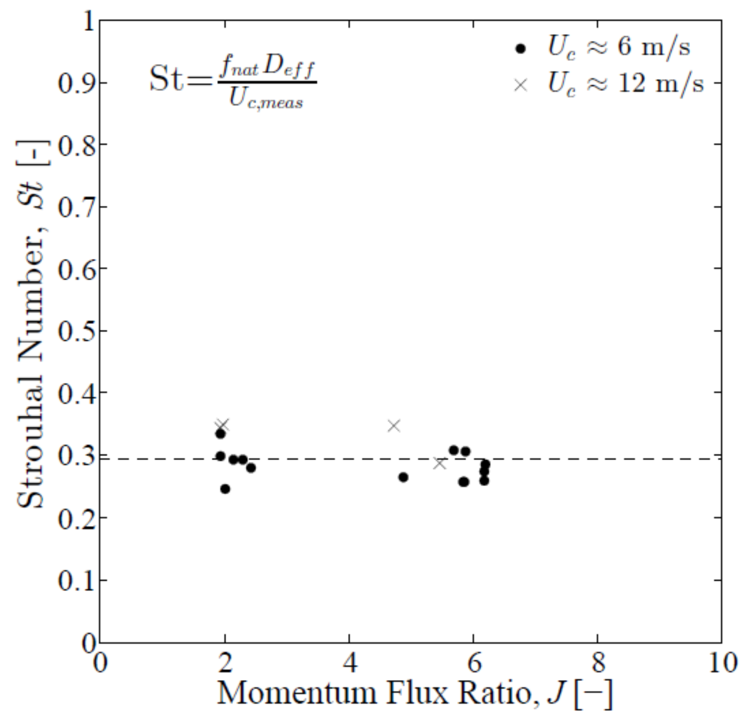

Pressure Antinode Response

$$A = \frac{p'}{\frac{1}{2}\rho_2 U_2^2}$$

$$J = 2.0$$

$$F = \frac{f_{forcing}}{f_{jet}} = 2.6$$

0.28 | 0.44 | 0.73 | 1.6 | 2.49 | 4.39 | 4.97

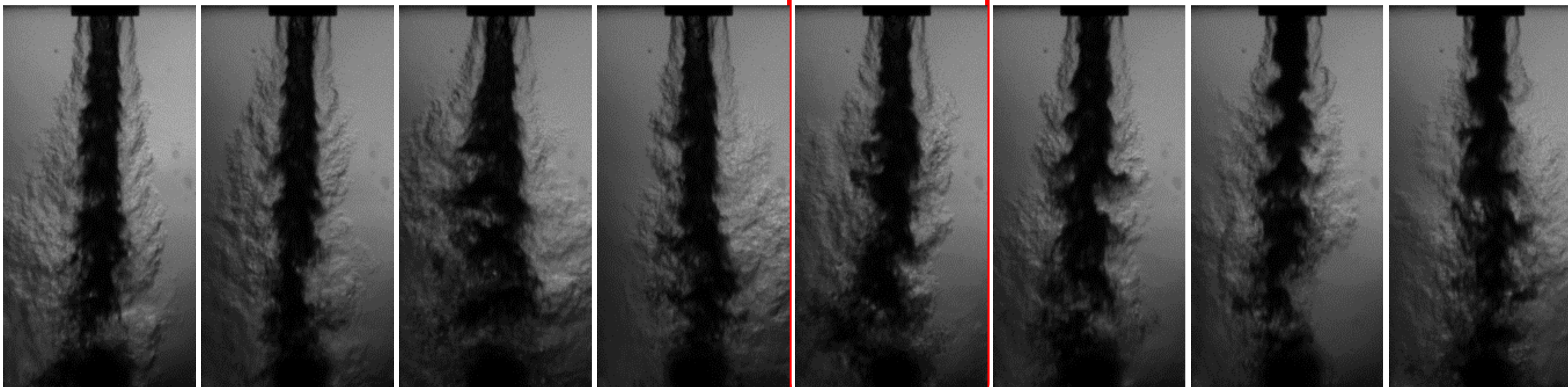

No receptivity

Weak receptivity

High receptivity

Natural convective POD mode pair

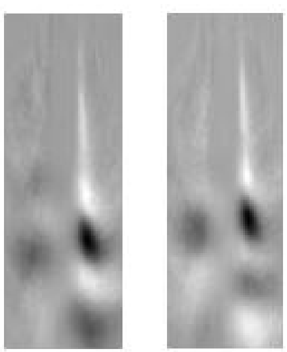

Forced convective POD mode pair

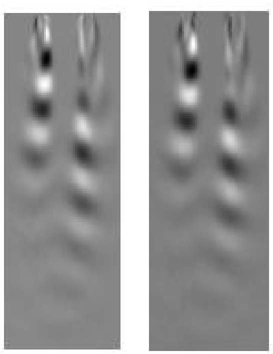

Pressure Antinode Mechanism

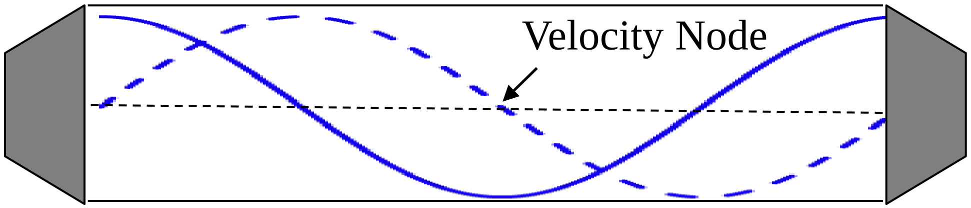

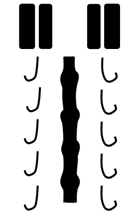

Outer jet mass flow pulsations

	POD structure	unforced	Max forcing	POD structure
J = 2		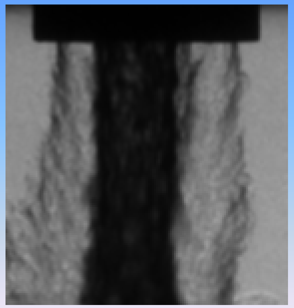	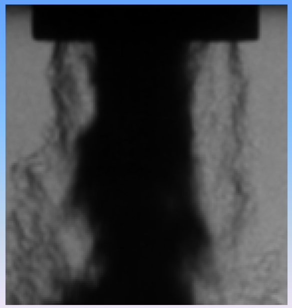	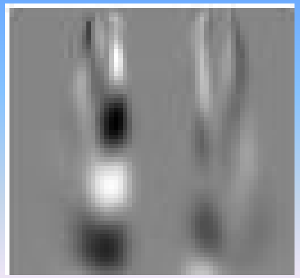
J = 6	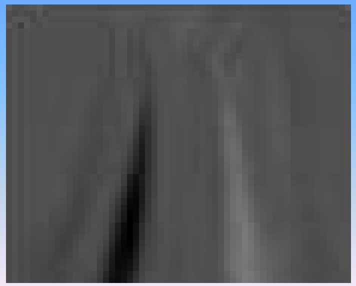		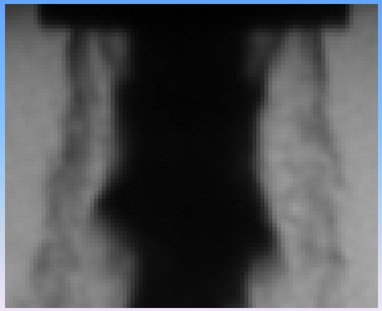	

Pressure Node Response

$J = 2.0$ $\qquad F = \dfrac{f_{forcing}}{f_{jet}} = 2.6$

U' = 0 | 0.06 m/s | 0.12 m/s | 0.16 m/s | 0.25 m/s | 0.34 m/s | 0.52 m/s | 0.72 m/s

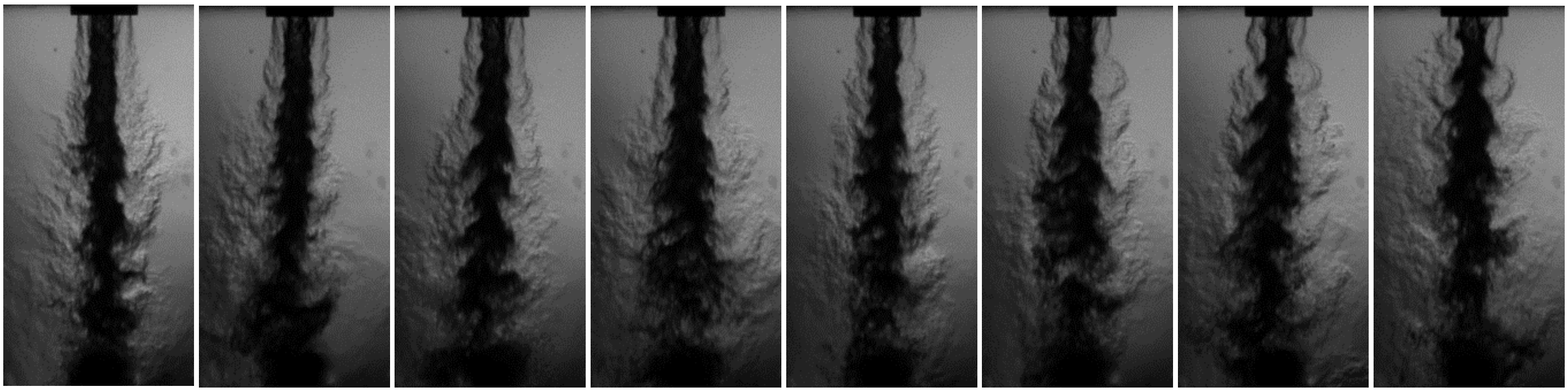

No receptivity

Weak receptivity

High receptivity

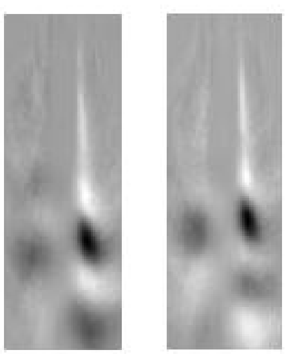

Natural convective POD mode pair

Forced convective POD mode pair

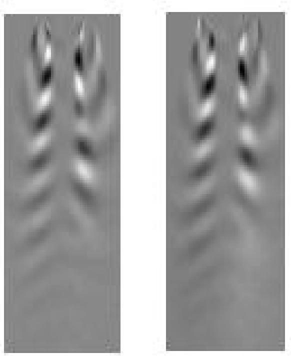

Pressure Node Mechanism

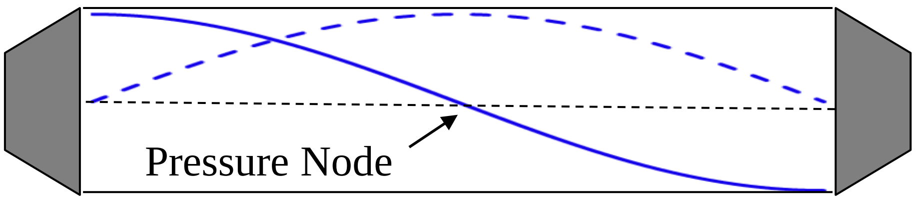

Apparent excitation of antisymmetric mode in the outer jet that drives instabilities in the inner jet

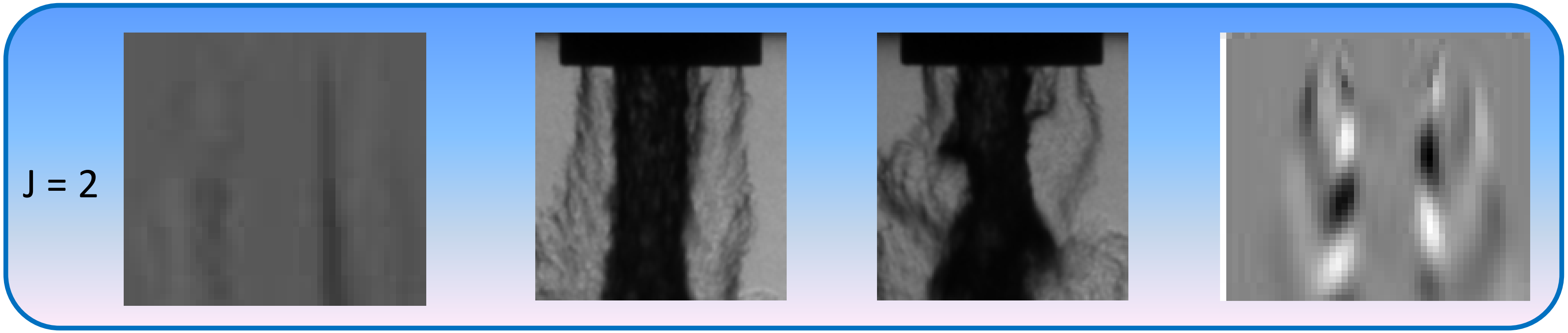

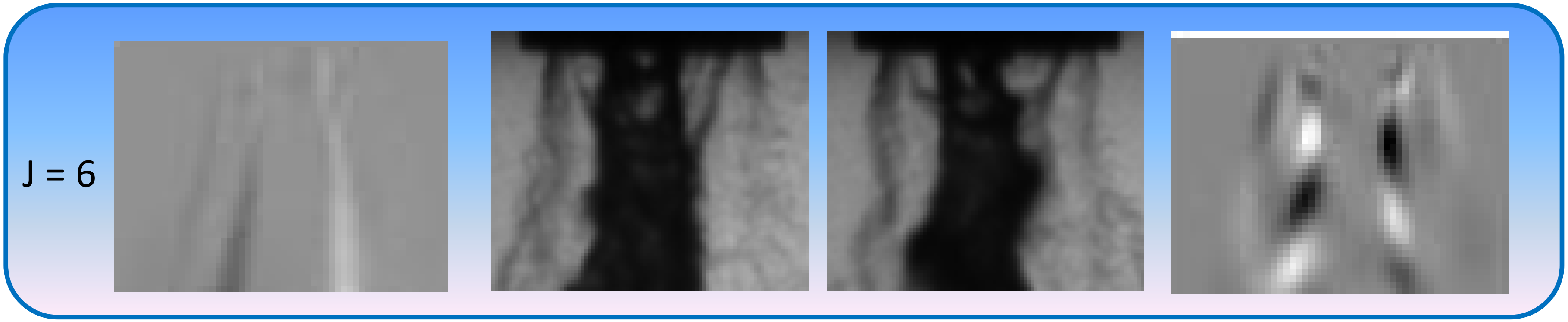

Summary and Future Work

- **AFRL ready to commence reacting flow experiments with acoustics**
- **Target specific injector conditions, and explore new forcing parameters (dimensionless frequency and amplitude)**
  - Identify natural frequencies of reacting coaxial jets
  - Determine forcing conditions at which the reacting flow is receptive to acoustics
  - Characterize the heat release response within the receptive regime
- **Preliminary cold flow "shakedown" data demonstrates receptivity dependency on frequency and amplitude**

Backup slides

Unforced Coaxial Jets

- **Frequency depends on location**

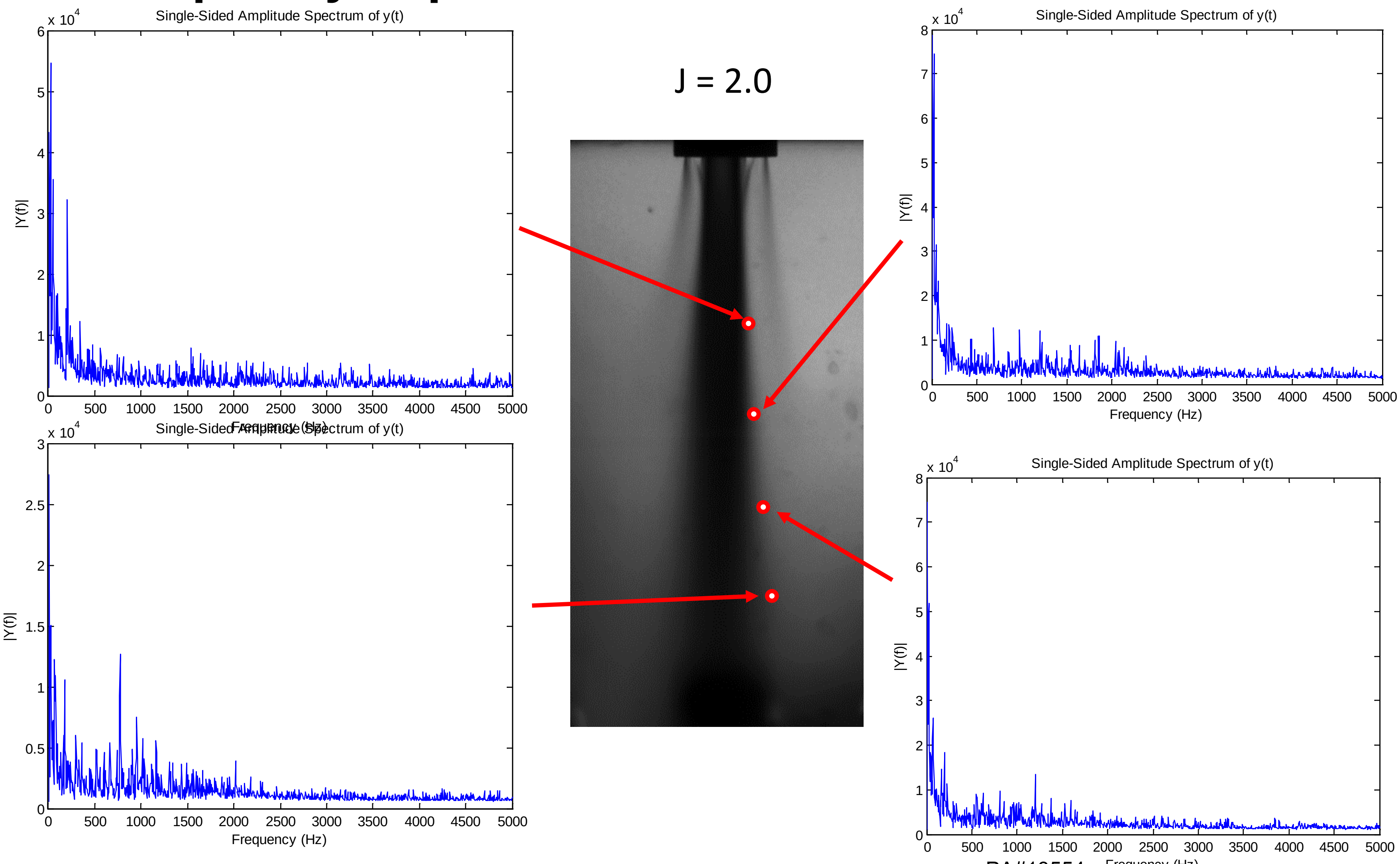

Convection Velocity

Convective Shear Layer Velocity by Dimotakis (1986)
Vortex Frame of Reference

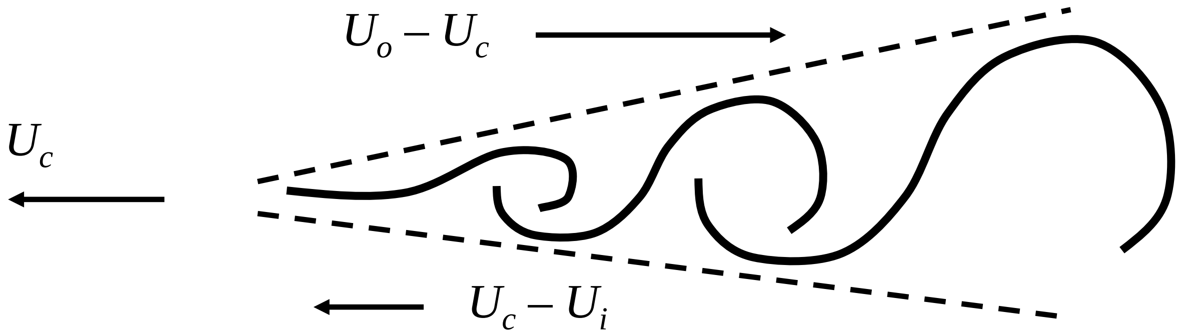

$(U_o > U_i)$

- Bernoulli's equation
  - A stagnation point must exist between vortices. Therefore, along a line through this point, dynamic pressures are approximately equal.

$$\rho_o(U_o - U_c) \approx \rho_i(U_c - U_i)$$

$$U_c = \frac{U_o \rho_o^{1/2} + U_i \rho_i^{1/2}}{\rho_o^{1/2} + \rho_i^{1/2}} \qquad St = \frac{f_{nat} D}{U_c}$$

$\Rightarrow$ If St, D, U_c are held constant then f_{nat} may be constant.

Frequency Dependence

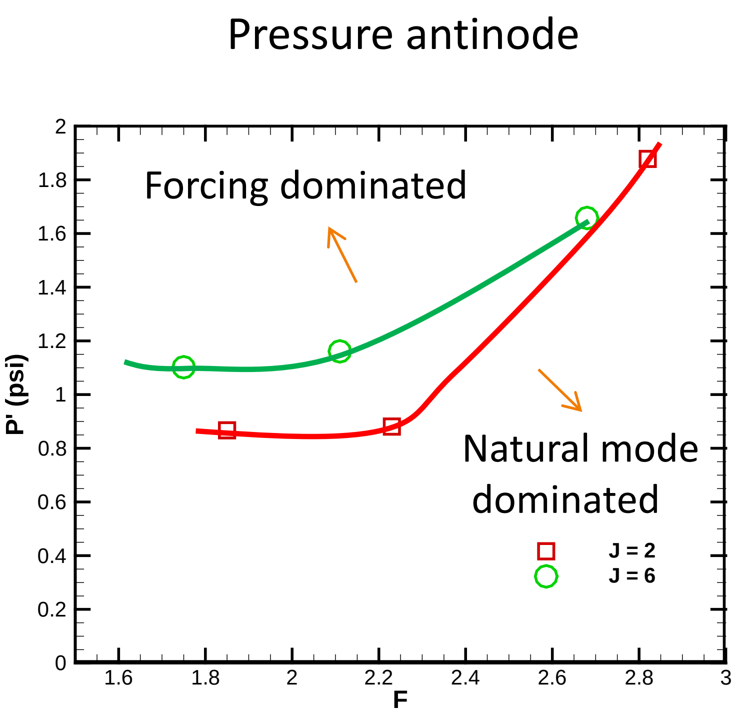

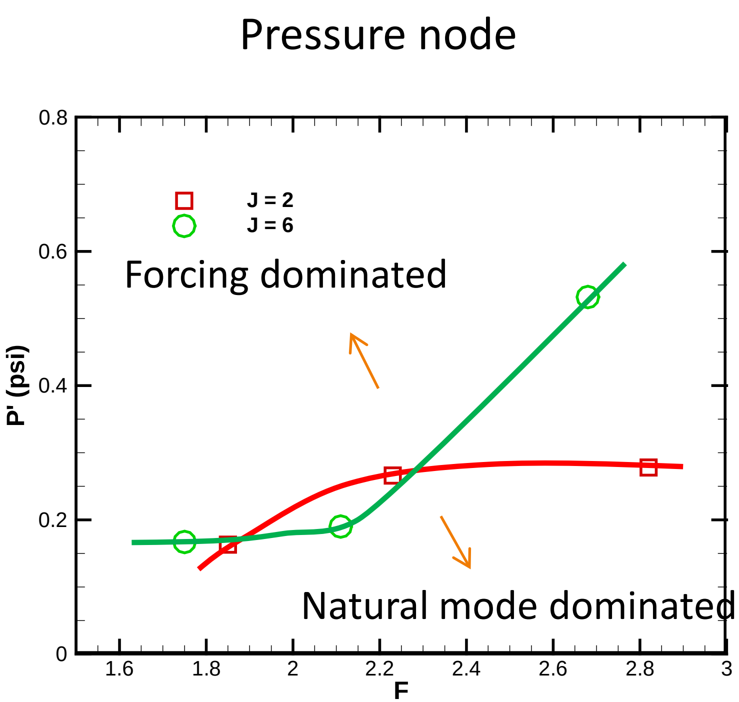

Convective Mode from POD

- Proper Orthogonal Decomposition
  - To identify traveling, coherent structures, a conjugate mode pair is identified as any two modes whose CPSD magnitude peaks near a phase of ±90°.[12]

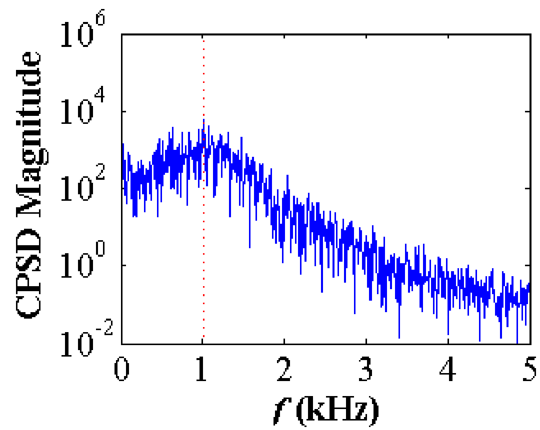

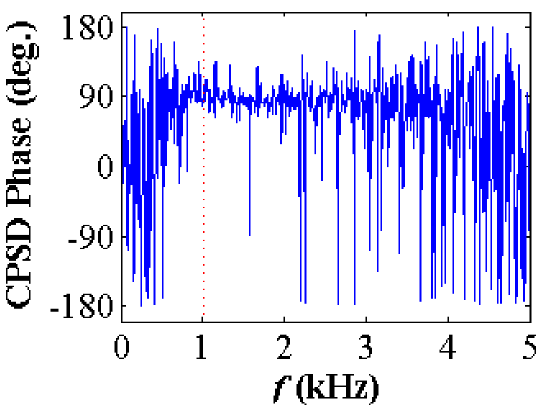

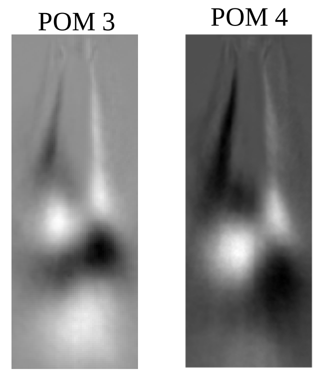

POMs 3 & 4 exhibit the same flow structure, shifted by 90° in the direction of flow.

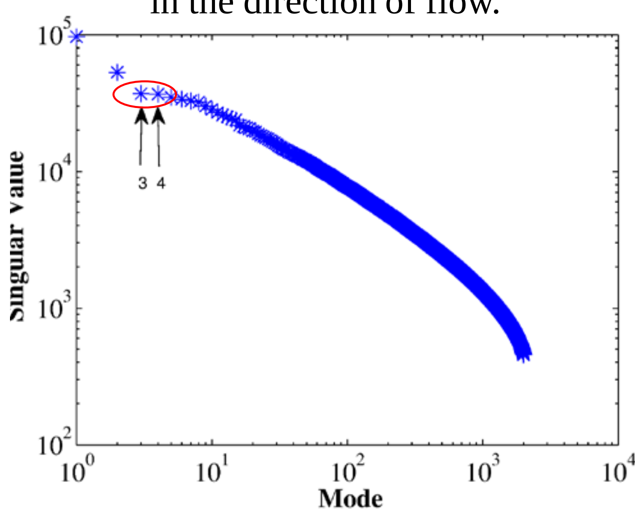

⇨ Proper orthogonal modes (POMs) 3 & 4 were found to be the **most energetic conjugate pair.**

⇨ The natural mode is represented by POMs 3 & 4.

⇨ The natural mode spans a band of frequencies rather than a single peak frequency.

Arienti, M. and Soteriou, M.C.(2009)